www.czasopisma.pan.pl PAN www.journals.pan.pl

Metrol. Meas. Syst., Vol. 23 (2016), No. 2, pp. 251–260.

METROLOGY AND MEASUREMENT SYSTEMS

Index 330930, ISSN 0860-8229

www.metrology.pg.gda.pl

CLASSIFICATION OF EEG SIGNALS USING ADAPTIVE TIME-FREQUENCY DISTRIBUTIONS

Nabeel A. Khan[1], Sadiq Ali[2]

1) Federal Urdu University, Department of Electrical Engineering, Khayaban-e-Suhrwardy Road, G-7, Islamabad, Pakistan (✉ nabeel.alikhan@gmail.com, +92 333 930 2491)

2) University of Engineering and Technology Peshawar, Department of Electrical Engineering, Peshawar, Pakistan (engsat@gmail.com)

Abstract

Time-Frequency (*t-f*) distributions are frequently employed for analysis of new-born EEG signals because of their non-stationary characteristics. Most of the existing time-frequency distributions fail to concentrate energy for a multicomponent signal having multiple directions of energy distribution in the *t-f* domain. In order to analyse such signals, we propose an *Adaptive Directional Time-Frequency Distribution* (ADTFD). The ADTFD outperforms other adaptive kernel and fixed kernel TFDs in terms of its ability to achieve high resolution for EEG seizure signals. It is also shown that the ADTFD can be used to define new time-frequency features that can lead to better classification of EEG signals, *e.g.* the use of the ADTFD leads to 97.5% total accuracy, which is by 2% more than the results achieved by the other methods.

Keywords: Adaptive Directional Time-Frequency Distribution, EEG signals, Time-Frequency features, Pattern recognition.

1. Introduction

EEG signals are widely used for detecting abnormalities such as seizure in new-borns. Most of the existing abnormality detection methodologies require visual analysis by a neurophysiologist. Detection of abnormality in EEG signal is a non-stationary signal classification problem that involves extraction of features from time-domain, frequency domain or joint *t-f* domain representations of signal [1–6]. Recent studies have indicated that EEG signals have non-stationary characteristics, so time-frequency methods are preferred tools for their analysis [2]. Typical *t-f* signal classification approaches can be classified into two categories: 1) template matching approaches, where a *t-f* representation of a given signal is correlated with stored templates to detect the presence of abnormality [7]; 2) machine learning approaches that involve such steps as feature extraction and classifier training [2]. The time-frequency features can be extracted by dimensionality reduction approaches such as singular value decomposition [2], interpreting TFDs as images and using texture information as features [8, 9], separating signal components using empirical mode decomposition and extracting features from the separated components [3, 5, 6].

Quadratic *Time-Frequency Distributions* (TFD) are frequently employed for analysis and extraction of features from EEG signals because of their high resolution [4]. The *Wigner-Ville Distribution* (WVD) is a core distribution of this class. It gives ideal resolution for mono-component *Linear Frequency Modulated* (LFM) signals, but suffers from the cross-term interference for multi-component and non-linear frequency modulated signals [11]. Cross-terms are oscillatory in nature and the frequency of oscillation increases as the distance between signal components is increased. Quadratic TFDs reduce cross-terms by convolving the WVD

Article history: received on Nov. 01, 2015; accepted on Jan. 26, 2016; available online on May 16, 2016, DOI: 10.1515/mms-2016-0021.

with a 2D smoothing kernel [11]. However, smoothing also deteriorates the energy concentration of auto-terms. Quadratic TFDs based on separable *t-f* kernels give a better compromise between the cross-term suppression and auto-term resolution because of the flexibility to independently adjust smoothing along time and frequency axes [11]. However, these methods fail to give the optimal energy concentration for signals whose auto-terms form an angle with the time axis in the *t-f* plane. In such scenarios, directional filtering schemes give better performance [12]. These methods employ one kernel for each point in the *t-f* plane and are not suitable for EEG signals that can have more than one direction of energy concentration in the *t-f* plane. Therefore, there is a need to develop an adaptive directional filtering technique that adapts the direction of smoothing kernel at each point in the *t-f* plane.

In this study, we propose a high resolution adaptive directional time-frequency distribution (ADTFD) that adapts the direction of its smoothing kernel at each point in the *t-f* plane resulting in a clear representation of spike as well as rhythmic characteristics of EEG seizure signals [13]. It is also shown that the better visual representation of EEG seizure signals can be used to develop a new *t-f* pattern recognition approach for the classification of EEG signals. This study extends our earlier work related to the feature extraction and TFD design in the following ways [2, 4, 13]:

1) It is demonstrated that the ADTFD, developed earlier in the context of instantaneous frequency estimation of synthetic signals, is a powerful tool for analysis and modelling of EEG seizure signals. It gives a very clear representation for signals with rhythmic as well as spike characteristics. Most of the previous studies using the *t-f* approach focused only on EEG seizure signals with the rhythmic activity, the spike characteristics being ignored [7, 10].
2) Effective modelling of EEG signals in the *t-f* domain helps in defining new features, such as the ones defined in Section 4, which can lead to better classification results. This study establishes a link between the resolution of a given TFD and its classification performance by illustrating that high resolution TFDs, such as the ADTFD, lead to better classification results.

The ADTFD is defined in section 2. Section 3 compares the state-of-the-art TFDs for analysis of EEG signals. Section 4 presents the methodology for extraction of features from high resolution TFDs. Section 5 presents the results of the proposed *t-f* pattern recognition for detection of abnormalities in EEG signals. Finally, section 6 concludes the paper.

2. Adaptive directional kernel time-frequency distribution

In this section, we present a high resolution TFD, which is obtained by adapting the direction of a smoothing kernel for each point in the *t-f* plane. The ADTFD is expressed as [13]:

$$\rho_{adaptive}(t,f) = \iint W_Z(t-t', f-f')\gamma_{\theta(t,f)}(t',f')dt'\,df', \tag{1}$$

$W_Z(t,f)$ is the WVD of the analytic signal $z(t)$, defined as:

$$W_z(t,f) = \int z(t+\tfrac{\tau}{2})z^*(t-\tfrac{\tau}{2})e^{-j2\pi f\tau}d\tau, \tag{2}$$

$\gamma_{\theta(t,f)}(t',f')$ is an adaptive kernel whose direction is adapted at each point in the *t-f* plane. In this study, we have selected the second order partial derivative of the *Directional Gaussian Filter* (DGF) as a directional kernel, which is widely used in image processing for the enhancement and extraction of ridges [14, 15]. It is defined as:

$$\gamma_{\theta_{(t,f)}}(t,f) = \frac{d^2}{dt_\theta^{\,2}}\left[e^{-\left(a^2 t_\theta^{\,2} + b^2 f_\theta^{\,2}\right)}\right],\ \ t_\theta = t\cos(\theta) + f\sin(\theta),\ \ f_\theta = -t\sin(\theta) + f\cos(\theta), \tag{3}$$

Metrol. Meas. Syst., Vol. 23 (2016), No. 2, pp. 251–260.

where θ is the rotation angle, and the parameters a and b control the spread of DGF along the time and frequency axes, respectively. The design criterion to choose the direction of DGF for each point in the *t-f* plane is based on the following observations [13]:

1) Filtering along the major axis of the auto-terms does not blur a TFD [10].
2) The direction of oscillation of cross-terms is along the major axis of cross-terms or the direction of energy distribution.

Therefore, adapting the direction of filter along the direction of maximum energy will suppress the cross-terms without affecting the resolution of the auto-terms. The direction of the maximum energy is thus the optimum angle for smoothing using the DGF, which can be estimated by maximizing its correlation with the absolute WVD [13]. This can be expressed as:

$$\hat{\theta}_{(t,f)} = \underset{\theta}{\arg\max}\left[\left|\iint \left|W_z(t-t',f-f')\right|^2 \gamma_{\theta_{(t,f)}}(t',f')dt'df'\right|^2\right], \tag{4}$$

3. Comparative analysis of TFDs used for analysing EEG signals

In this section, we compare the performance of the ADTFD with other standard quadratic TFD in terms of its ability to analyse EEG seizure signals. For numerical comparison of methods, we used a model synthetic signal and a real-life EEG. Most of the EEG signals can be classified into the following categories based on the visual analysis of *t-f* patterns of these signals.

1) Signals with both rhythmic and spike characteristics.
2) Signals with the rhythmic activity.

3.1. Signal composed of sinusoid and spike

Signals that have both rhythmic and spike characteristics are difficult to analyze using the existing methods of *t-f* analysis. These signals have two directions of energy distribution: one along the time axis because of the rhythmic activity, and another − along the frequency axis because of the spikes. In order to reduce the cross-terms generated by spikes, smoothing must be performed along the frequency axis, but such smoothing will reduce the resolution of sinusoidal signal component. In order to obtain a high-resolution *t-f* representation for all components of such signals, the adaptive optimization of *t-f* kernel is needed at each *t-f* point.

Synthetic Signal: we first consider a synthetic, sinusoidal spiky signal given below.

$$s(t) = s_1(t)+s_2(t)+s_3(t)+s_4(t)+s_5(t)+s_6(t)+s_7(t), \tag{5}$$

where:

$$s_1(t) = \cos(3.2\pi t), \tag{6}$$

$$s_2(t) = e^{-\left(\frac{t-0.9375}{0.0447}\right)^2}, \tag{7}$$

$$s_3(t) = e^{-\left(\frac{t-2.1875}{0.0447}\right)^2}, \tag{8}$$

$$s_4(t) = e^{-\left(\frac{t-3.4375}{0.0447}\right)^2}, \tag{9}$$

$$s_5(t) = e^{-\left(\frac{t-4.6875}{0.0447}\right)^2}, \tag{10}$$

$$s_6(t) = e^{-\left(\frac{t-5.9375}{0.0447}\right)^2}, \tag{11}$$

$$s_7(t) = e^{-\left(\frac{t-7.1875}{0.0447}\right)^2}. \tag{12}$$

This signal is sampled at 32 Hz and has the duration of 8 s. The signal is high-pass filtered with the frequency cut-off of 0.05 *Hz*. In order to get the true representation of the signal, each signal component is analyzed separately using the WVD, and then the WVDs of signal components are added up to obtain a cross-term-free high-resolution TFD, which will be used as the reference for comparison. The synthetic multi-component signal is analyzed using the ADTFD [14], *Extended Modified B Distribution* (EMBD) [2], *Multi-Directional Distribution* (MDD) [2], spectrogram, and the true *t-f* representation (computed by adding WVDs of signal components), as illustrated in Fig. 1. We have optimized parameters of all the TFDs based on visual inspection to maximize the energy concentration of auto-terms while minimizing their cross-terms. Fig. 1 shows that the ADTFD is closest to the ideal *t-f* distribution because of the adaptive optimization of its parameters at each *t-f* point. It gives a highly concentrated *t-f* representation of both spikes and sinusoid while other distributions have failed to concentrate energy for both spikes and sinusoid.

Original Signal: A sinusoidal spiky real-life EEG signal is being analyzed using the ADTFD, EMBD, *Multi-Directional Distribution* (MDD), and spectrogram, as illustrated in Fig. 2. We have optimized parameters of all the TFDs based on visual inspection to maximize their resolution while minimizing cross-terms. The ADTFD gives a highly concentrated *t-f* representation because of the adaptive optimization of its kernel at each t-f point, while all other TFDs have failed to concentrate energy.

3.2. EEG seizure signals with rhythmic activity

EEG seizure signals with the rhythmic activity can be modelled as a summation of multiple linear frequency modulated chirps of varying amplitudes and chirp rates. Such signals can have multiple directions of energy concentration in the *t-f* plane, so one kernel cannot give the optimal energy concentration for all the signal components.

Synthetic Signal: In order to validate the performance of the ADTFD, we first consider a synthetic multi-component signal of varying amplitudes and chirp rates.

$$s(t) = s_1(t) + s_2(t) + 0.65 s_3(t) + 0.35 s_4(t) + 0.35 s_5(t), \tag{13}$$

where:

$$s_1(t) = \cos\left(2\pi\left(0.0067(t-4)^4 + 1.6t\right)\right), \tag{14}$$

$$s_2(t) = \cos\left(2\pi\left(0.0067(t-4)^4 + 3.2t\right)\right), \tag{15}$$

$$s_3(t) = \cos\left(2\pi\left(0.0182(t-4)^4 + 6.4t\right)\right), \tag{16}$$

$$s_4(t) = \cos\left(2\pi\left(0.0182(t-4)^4 + 9.6t\right)\right), \tag{17}$$

$$s_5(t) = \cos\left(2\pi\left(0.0286(t-4)^4 + 12.8t\right)\right). \tag{18}$$

The signal has the 8 s duration and is sampled at 32 Hz. This signal is analysed using the ADTFD, EMBD, MDD, and spectrogram, as illustrated in Fig. 3. The ADTFD gives a clear

Metrol. Meas. Syst., Vol. 23 (2016), No. 2, pp. 251–260.

representation of all signal components including signal components of low amplitudes while other TFDs have failed to concentrate energy for such low amplitude signal components.

Original Signal: a real-life EEG signal with multi-component characteristics is being considered. The signal is analysed using the EMBD, ADTFD, spectrogram and MDD, as shown in Fig. 4. The ADTFD gives a high energy concentration of both low-amplitude high-frequency signal components and high-energy low-frequency components, while other TFDs have failed to give a clear representation for the low-amplitude signals.

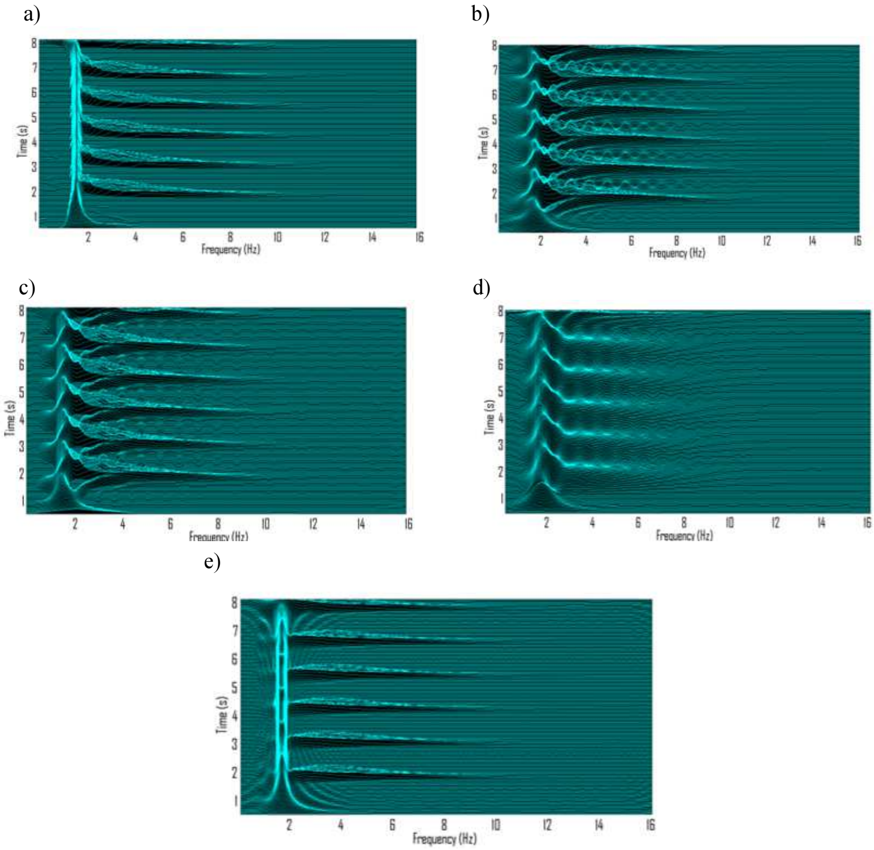

Fig. 1. The time-frequency analysis of a synthetic signal composed of both a sinusoid and spikes.
a) The ADTFD (a = 3, b = 12); b) the EMBD ($\alpha = 0.1$, $\beta = 0.2$); c) the MDD ($\theta_1 = 0^0$, $\theta_2 = 90^0$, $E_1 = 0.1$, $E_2 = 0.45$, D = 0.05); d) the spectrogram (Hamming window of length 61); e) the true TFD.

4. Time-frequency features for classification of EEG signals

4.1. Observation from time-frequency images

We have the following observations regarding the time-frequency characterization of EEG seizure signals.

1. Many EEG signals can be modelled as multi-component signals of varying amplitudes and chirp rates. These signals can be characterized by the *Instantaneous Frequency* (IF) and *Instantaneous Amplitude* (IA) of signal components. Therefore, the IF and IA of signal components will be used for extracting features for the classification of EEG signals.

2. The energy of EEG seizure signals in the *t-f* plane is either parallel to the time axis due to the rhythmic activity, as shown in Fig. 2, or parallel to the frequency axis due to the spike characteristics, as shown in Fig. 4. This implies that the signal energy is not distributed along the diagonal axis for EEG seizure signals. This information can be exploited for the detection of seizure activity by estimating the rate of change of signal energy along the diagonal axis.

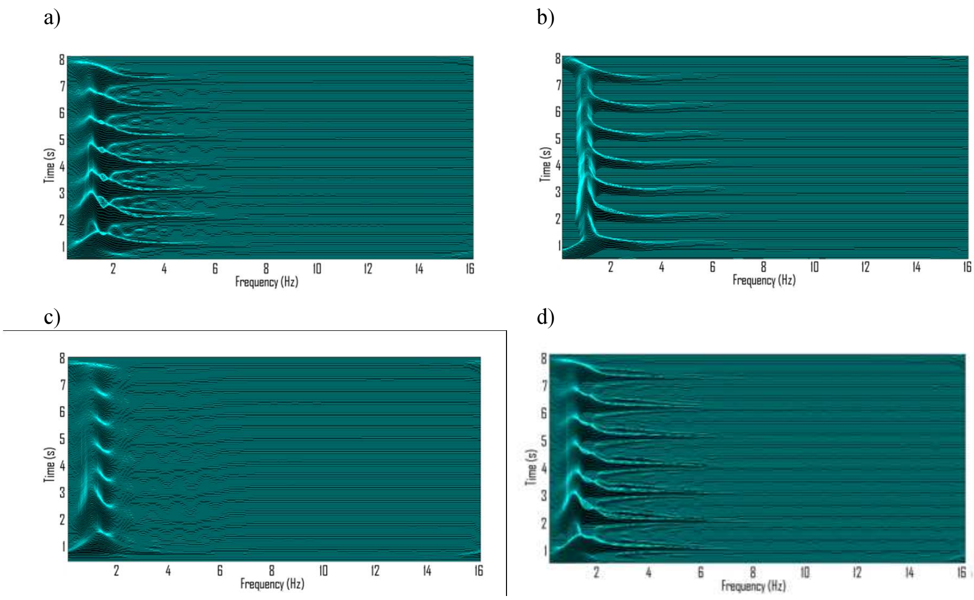

Fig. 2. The time-frequency analysis of a real-life new-born EEG seizure signal composed of both a sinusoid and spikes. a) The EMBD ($\alpha = 0.1$, $\beta = 0.2$); b) the ADTFD (a = 3, b = 12); c) the spectrogram (Hamming window of length 61); d) the MDD ($\theta_1 = 0^0$, $\theta_2 = 90^0$, $E_1 = 0.1$, $E_2 = 0.45$, D = 0.05).

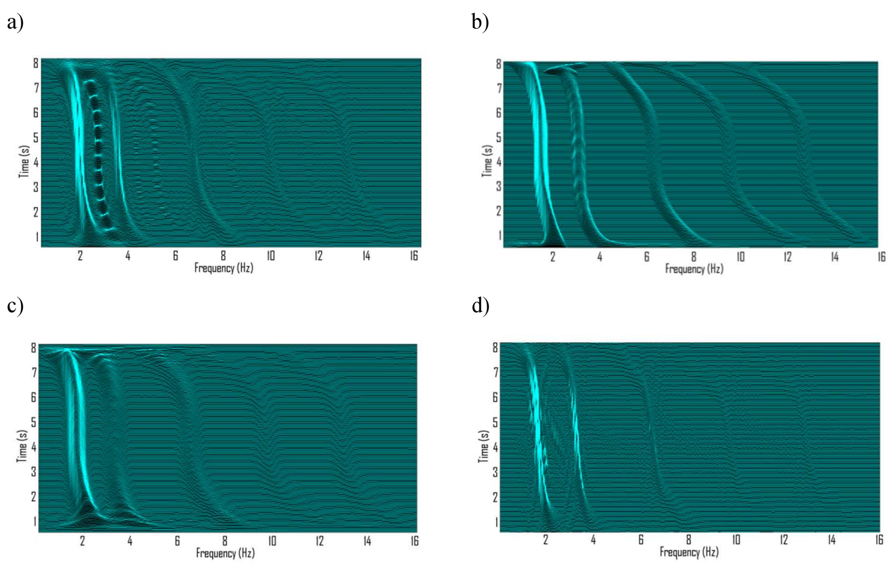

Fig. 3. Analysis of the synthetic multi-component signal using TFDs.
a) The EMBD; b) the ADTFD (a = 3, b = 12); c) the spectrogram (Hamming window of length 85);
d) the MDD ($\theta = 0$, c = 0.1, $D = 0.02$, $E = 0.1$).

Metrol. Meas. Syst., Vol. 23 (2016), No. 2, pp. 251–260.

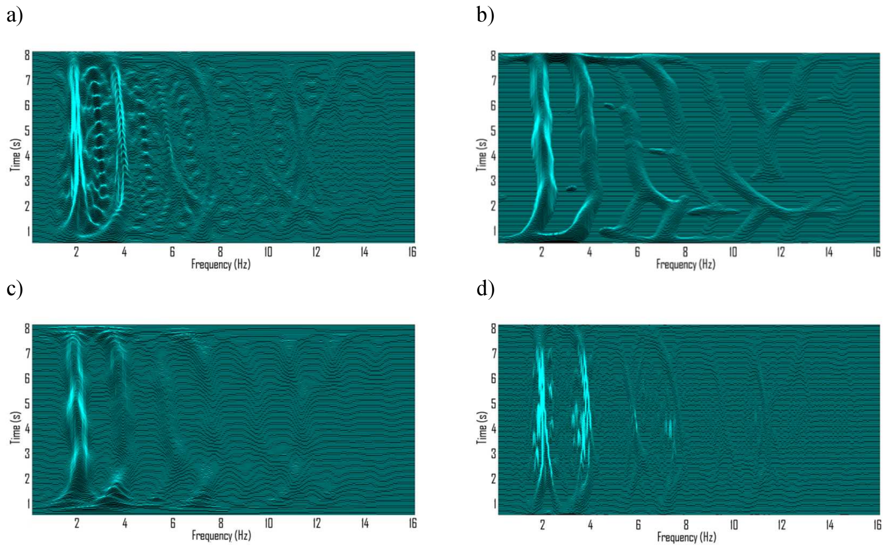

Fig. 4. The time-frequency representations of EEG signals. a) The EMBD ($\alpha = 0.1$, $\beta = 0.2$); b) the ADTFD (a = 3, b = 12); c) the spectrogram (Hamming window of length 85); d) the MDD ($\theta = 0$, c = 0.1, $D = 0.02$, $E = 0.1$).

4.2. Instantaneous Frequency (IF)- and Instantaneous Amplitude (IA)-related features

The IF of a mono-component signal is defined as the location of the peak frequency in the *t-f* plane [16]:

$$f(t) = \arg\max_{f} [\rho(t, f)]. \tag{19}$$

The IA of a mono-component signal is defined as the amplitude of the peak frequency in the *t-f* plane [16]:

$$a(t) = \rho(t, f(t)). \tag{20}$$

However, the above mentioned definitions are valid only for mono-component signals. In order to extend them for multi-component signals, the following procedure has been applied:

1. Initialize $i = 1$.
2. Estimate the IF of the i-th signal component:

$$f_i(t) = \arg\max_{f} [\rho(t, f)]. \tag{21}$$

3. Estimate the IA of the i-th signal component:

$$a_i(t) = \rho(t, f_i(t)). \tag{22}$$

4. Set all points in the region around the estimated IF to zero:

$$\rho(t, f) = 0. \quad for\ f_i(t) - B \le f \le f_i(t) + B\,. \tag{23}$$

5. Increment $i = i + 1$. Repeat from 2 till 'i' becomes equal to 4.

Note that the procedure described in (21) to (23) can be related to the *Empirical Mode Decomposition* (EMD)-based procedure of signal component extraction [3]. However, the aforementioned procedure based on quadratic TFDs offers a higher resolution as compared with the EMD, as has been shown in previous studies [17]. The IF and IA cannot be directly used as a feature for classification since that will increase the dimensionality of problem. Nevertheless, we can extract such features as the average frequency and average amplitude from the IF and IA of multi-component signals, as shown in Table 1. In this study, the signal duration of 8 s is used to estimate the IF- and IA-related features.

Table 1. The IF- and IA-related statistical features for classification of EEG signals.

Feature	Formula
Mean of the IF	$F_{1_i} = \frac{1}{T}\int_0^T f_i(t)dt$
Mean of the IA	$F_{2_i} = \frac{1}{T}\int_0^T a_i(t)dt$
Variance of the IF	$F_{3_i} = \sigma_{f_i}^2 = \frac{1}{T}\int_0^T \left(f_i(t) - \frac{1}{T}\int_0^T f_i(t)dt \right)^2 dt$
Variance of the IA	$F_{4_i} = \sigma_{a_i}^2 = \frac{1}{T}\int_0^T \left(a_i(t) - \frac{1}{T}\int_0^T a_i(t)dt \right)^2 dt$
Kurtosis of the IF	$F_{5_i} = \frac{1}{\sigma_{f_i}^2 T}\int_0^T \left(f_i(t) - \frac{1}{T}\int_0^T f_i(t)dt \right)^4 dt$
Kurtosis of the IA	$F_{6_i} = \frac{1}{\sigma_{a_i}^2 T}\int_0^T \left(a_i(t) - \frac{1}{T}\int_0^T a_i(t)dt \right)^4 dt$

4.3. Energy in high frequencies of t-f images

Analysis of EEG seizure signals using the ADTFD has revealed that the EEG seizure signals appear either as multi-component signals with slow variation in its IF or as a sinusoidal spiky signal. In the first case, the direction of signal energy is parallel to the time axis while in the second case the direction of signal energy is parallel to the frequency axis. So, the seizure signals do not have distributions of signal energy along the diagonal axis in the *t-f* plane. In order to exploit this information, the rate of change of signal energy along the diagonal axis in the *t-f* plane normalized by the total energy of a given *t-f* image can be used as a feature. The rate of change of signal energy along the diagonal axis can be estimated by differentiating the given TFD along both time and frequency axes.

$$F_7 = \frac{\iint \left| \frac{d}{dt}\frac{d}{df}\rho(t,f) \right| dtdf}{\iint \left| \rho(t,f) \right| dtdf} . \tag{24}$$

5. Results and discussion

The *t-f* features described earlier are used to classify neonatal EEG signals. In this study, we have used the two following classes: 1) EEG signals with the seizure activity; 2) EEG signals with the non-seizure activity. These neonatal EEG seizure signals were acquired from 5 neonates and were labelled by an expert neurophysiologist. Further details of this database are given in [2]. A set of 200, 8 s epochs of new-born EEG background and a set of 200, 8 s epochs of new-born EEG seizure is randomly extracted from this database. The length of each segment of database is 256 samples (with the sampling frequency of 32 Hz). In order to extract EEG

Metrol. Meas. Syst., Vol. 23 (2016), No. 2, pp. 251–260.

features, each segment is analysed by selected TFDs; these are: the EMBD, Spectrogram (SPEC), Smoothed WVD (SWVD), ECSK, adaptive TFD and WVD.

The maximum relevance and minimum redundancy criterion is applied to select the optimal subsets of features from the above mentioned sets of features [18]. These optimal subsets of features are then used to train the linear support vector machine (SVM) classifiers. The results are estimated using the leave-one-out fold cross-validation procedure; this procedure uses one sample for testing while the remaining samples are used for training. This procedure is repeated for each sample in the database, so that each sample is used once for validation. The results are presented in terms of the sensitivity, specificity, and total accuracy, in Table 2. These measures are defined as follows:

$$\text{Sensitivity} = \frac{\text{True Positive}}{\text{Total Number of True Positives}}, \tag{25}$$

$$\text{Specificity} = \frac{\text{True Negative}}{\text{Total Number of True Negatives}}, \tag{26}$$

$$\text{Total Accuracy} = \frac{\text{True Positive} + \text{True Negative}}{\text{Total Number of Examples}}. \tag{27}$$

True positive is the case when a classifier correctly detects the seizure segment, whereas true negative is the case when a given classifier correctly detects the non-seizure segment.

The best classification results with the total accuracy of 97.5% for the proposed *t-f* pattern recognition technique are obtained using the ADTFD. The proposed approach is computationally expensive as compared with the conventional time-only or frequency-only approaches because of the additional step required to transform a given signal from the time domain onto the *t-f* domain. However, the computational cost of the proposed methodology is less likely to affect its real-time implementation, given that EEG signals are low-frequency signals and most of the useful information is below 16 Hz.

Table 2. The classification accuracy results for new-born EEG data.

TFD	Sensitivity	Specificity	Total Accuracy
WVD	90.50	93. 50	92.00
Spectrogram	94.5	89.00	91.75
EMBD	97.00	94.50%	95.75
ADTFD	99	96.00%	97.5%

6. Conclusions

A new time-frequency pattern recognition technique for classification of EEG signals based on extracting the *Instantaneous Frequency* (IF)- and *Instantaneous Amplitude* (IA)-related features from the *Time-frequency* (*t-f*) *Distributions* (TFD) is presented. In order to improve the accuracy of the IF and IA estimation algorithms, a high resolution *Data Adaptive Directional* TFD (ADTFD), based on adapting the direction of its smoothing kernel at each point in the *t-f* plane, is defined. The ADTFD is an effective tool for the analysis and classification of EEG seizure signals as it gives a close to ideal energy concentration for EEG seizure signals in the time-frequency domain as well as the best total classification accuracy of 97.5%.

Acknowledgements

This research has been partially supported by Qatar Foundation Grant NPRP 4-1303-2-517 and NPRP 6-885-2-364.

References

[1] Joshi, V., Pachori, R.B., Vijesh, A. (2014). Classification of ictal and seizure-free EEG signals using fractional linear prediction. *Biomedical Signal Processing and Control*, 9, 1–5.

[2] Boashash, B., Khan, N., Ben-Jabeur, T. (2015). Time-frequency features for pattern recognition using high resolution TFDs: A tutorial review. *Digital Signal Processing*, 40, 1–30.

[3] Sharma, R., Pachori, R.B. (2015). Classification of epileptic seizures in EEG signals based on phase space representation of intrinsic mode functions. *Expert Systems with Applications*, 42(3), 1106–1117.

[4] Boashash, B., Azemi, G., Khan, N. (2015). Principles of time-frequency feature extraction for change detection in non-stationary signals: Application to newborn EEG abnormalitiy detection. *Pattern Recognition*, 48(3), 616–627.

[5] Sharma, R., Pachori, R.B., Acharya, U.R. (2015). Application of Entropy Measures on Intrinsic Mode Functions for the Automated Identification of Focal Electroencephalogram Signals. *Entropy*, 17(2), 669–691.

[6] Fu, K., Qu, J., Chai, Y., Zou, T. (2015). Hilbert marginal spectrum analysis for automatic seizure detection in EEG signals. *Biomedical Signal Processing and Control*, 18, 179–185.

[7] Boashash, B., Azemi, G. (2014). A review of time–frequency matched filter design with application to seizure detection in multichannel newborn EEG. *Digital Signal Processing*, 28, 28–38.

[8] Wang, K.C. (2015). Time-Frequency Feature Representation Using Multi-Resolution Texture Analysis and Acoustic Activity Detector for Real-Life Speech Emotion Recognition. *Sensors*, 15(1), 1458–1478.

[9] Sameh, S., Lachiri, Z. (2012). Multiclass Support Vector Machines for Environmental Sounds Classification Using log Gabor Filters. *World Academy of Science, Engineering and Technology*, 6(8), 1185–1189.

[10] Abdulla, W., Wong, L. (2011). Neonatal EEG signal characteristics using time frequency analysis. *Physica A: Statistical Mechanics and its Applications*, 390(6), 1096–1110.

[11] Boashash, B. (2015). *Time-Frequency Signal Analysis and Processing: A Comprehensive Reference*. 2nd ed., Elsevier.

[12] Bastiaans, M., Alieva, T., Alieva, L. (2002). On Rotated Time-Frequency Kernels. *IEEE Signal Processing Letters*, 9(11), 378–381.

[13] Khan, N., Boashash, B. (2015). Multi-component instantaeous frequency estimation using locally adaptive directional time frequency distributions. *International Journal of Adaptive Control and Signal Processing*, DOI: 10.1002/acs.2583.

[14] Liu, Y., Mejias, L., Li, Z. (2012) Fast Power Line Detection and Localization Using Steerable Filter for Active UAV Guidance. *XXII Congress of the International Society for Photogrammetry, Remote Sensing*, Melbourne.

[15] Jacob, M., Unser, M. (2004). Design of steerable filters for feature detection using canny-lie criteria. *IEEE Transactions on Pattern Analysis and Machine Intelligence*, 26(8), 1007–1019.

[16] Boashash, B. (1992). Estimating and interpreting the instantaneous frequency of a signal. I. Fundamentals. *Proc. of the IEEE*, 80(4), 520–538.

[17] Auger, F., Flandrin, P., Lin, Y.T., McLaughlin, S., Meignen, S., Oberlin, T., Wu, H.T. (2013). Time-frequency reassignment and synchrosqueezing: An overview. *IEEE Signal Processing Magazine*, 30(6), 32–41.

[18] Peng, H., Long, F., Ding, C. (2005). Feature selection based on mutual information criteria of max-dependency, max-relevance, and min-redundancy. *IEEE Transactions on Pattern Analysis and Machine Intelligence*, 27(8), 1226–1238.